Smart Mater. Struct. **6** (1997) 491–497. Printed in the UK PII: S0964-1726(97)84464-3

TECHNICAL NOTE

Design and testing of a 1/12th-scale solid state adaptive rotor

Ron Barrett and James Stutts

Auburn University, Aerospace Engineering Department, Adaptive Aerostructures Laboratory, 211 Aerospace Engineering Building, Auburn, AL 36849-5338, USA

Received 6 January 1997, accepted for publication 9 May 1997

Abstract. A new approach to helicopter flight control through active blade pitch manipulation is presented. By using piezoceramic directionally attached piezoelectric (DAP) torque plates mounted between the rotor shaft and the blade root, the pitch angle of the helicopter rotor blades may be adjusted as the blades sweep the azimuth. Analytical models based on classical laminated plate theory for steady torque-plate deflection are presented. To verify the models, a 1/12th-scale two-bladed experimental test article was constructed. The test article was Froude scaled with a 122 cm total diameter and a 5.5 cm chord. Static and dynamic testing showed that blade pitch deflections could be controlled from −4 through +12° with good correlation between theory and experiment. Dynamic testing demonstrated that the first natural frequency in pitch was greater than 2.5 rev^{-1} with a maximum power consumption of 194 mW under the most extreme conditions, thus making it feasible for control of collective, longitudinal and lateral cyclic. Whirl-stand testing at up to 600 RPM showed that the rotor could generate thrust coefficients ranging from −0.0046 through +0.014 with little sensitivity of blade deflection to increases in rotor speed.

Nomenclature

A	extensional stiffness matrices	(N m^{-1})
B	coupling stiffness matrices	(N)
D	bending stiffness matrices	(N m)
C_T	thrust coefficient	—
E_3	through-thickness electric field	(V mm^{-1})
E	element stiffness	(GPa)
I_θ	blade section inertia about the feathering axis	
K_q	effective spring constant about the feathering axis	
L	length	(m)
m	mass density	
M	applied moment vector	(N m m^{-1})
N	applied force vector	(N m^{-1})
OR	orthotropy ratio $= E_L/E_T$	—
p–p	peak-to-peak	(var.)
t	thickness	(mm)
ΔT	temperature change	(°C)
T	thickness ratio $= t_s/t_a$	—
x	nondimensional radius	—
z	through-thickness dimension	(m)
α	coefficient of thermal expansion	(μstrain °C^{-1})
β	coning angle	
ε	laminate strain	(μstrain)
κ	laminate curvature	(rad m^{-1})
Λ	ith direction actuator free strains	(μstrain)
ν	Poisson's ratio	—
σ	stress	(MPa)
θ	blade pitch angle	(°)
Ω	angular speed	

Subscripts

1	longitudinal	2	lateral
a	actuator	b	bond
eff	effective	L	longitudinal
s	substrate	T	transverse

CAP	conventionally attached piezoelectric
DAP	directionally attached piezoelectric
HHC	higher harmonic control
IBC	individual blade control
IDE	interdigitated electrode
PFC	piezoelectric fiber composites
SSAR	solid state adaptive rotor

1. Introduction

The past 10 years have seen many studies on the fundamental characteristics, application principles and system designs of adaptive materials and structures.

0964-1726/97/040491+07$19.50

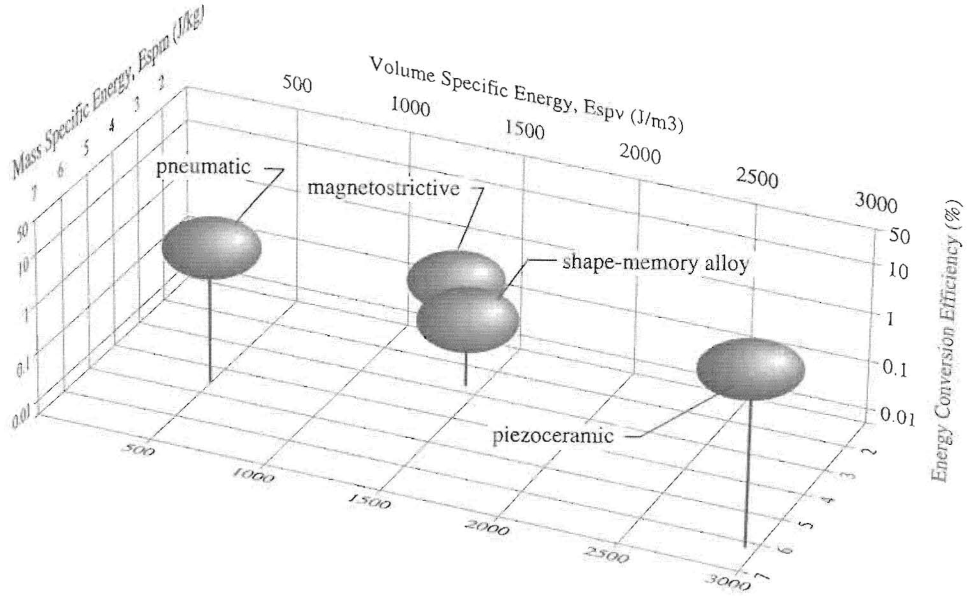

Figure 1. A mass, volume, energy and efficiency comparison of flight control actuator systems over a simulated 60 s flight of a FOG-M missile [1–3].

The applied forces and moments are given by

$$N = \int \sigma \, \mathrm{d}z \qquad M = \int \sigma z \, \mathrm{d}z. \tag{2}$$

If some of the limiting conditions such as actuator symmetry are applied, then an expression for the performance of a torque plate composed of DAP elements at 45° bonded to an isotropic substrate may be obtained. From [8], it can be seen that the twist deflections are maximized when the active elements are oriented at 45° and energized out of phase by 180°.

$$\begin{bmatrix} A_{11} & A_{12} & 2A_{16} & 0 & 0 & 0 \\ A_{12} & A_{22} & 2A_{26} & 0 & 0 & 0 \\ A_{16} & A_{26} & 2A_{66} & 0 & 0 & 0 \\ 0 & 0 & 0 & B_{11} & B_{12} & 2B_{16} \\ 0 & 0 & 0 & B_{12} & B_{22} & 2B_{26} \\ 0 & 0 & 0 & B_{16} & B_{26} & 2B_{66} \end{bmatrix}_a \begin{Bmatrix} \alpha_a \, \Delta T \\ \alpha_a \, \Delta T \\ 0 \\ \frac{\Lambda_1+\Lambda_2}{2} \\ \frac{\Lambda_1+\Lambda_2}{2} \\ \frac{\Lambda_1-\Lambda_2}{2} \end{Bmatrix} + \begin{Bmatrix} N_{11} \\ N_{22} \\ N_{12} \\ M_{11} \\ M_{22} \\ M_{12} \end{Bmatrix}_{ex} + \begin{bmatrix} (A_{11}+A_{12})_s \alpha_s \, \Delta T \\ (A_{11}+A_{12})_s \alpha_s \, \Delta T \\ 0 \\ 0 \\ 0 \\ 0 \end{bmatrix}$$

$$= \begin{bmatrix} A_{11} & A_{12} & 2A_{16} & B_{11} & B_{12} & 2B_{16} \\ A_{12} & A_{22} & 2A_{26} & B_{12} & B_{22} & 2B_{26} \\ A_{16} & A_{26} & 2A_{66} & B_{16} & B_{26} & 2B_{66} \\ B_{11} & B_{12} & 2B_{16} & D_{11} & D_{12} & 2D_{16} \\ B_{12} & B_{22} & 2B_{26} & D_{12} & D_{22} & 2D_{26} \\ B_{16} & B_{26} & 2B_{66} & D_{16} & D_{26} & 2D_{66} \end{bmatrix}_l \begin{Bmatrix} \varepsilon_{11} \\ \varepsilon_{22} \\ \varepsilon_{12} \\ \kappa_{11} \\ \kappa_{22} \\ \kappa_{12} \end{Bmatrix}. \tag{3}$$

Equation (3) has been shown to be generally accurate to within 5% of any generic torque plate. Significant deviations occur, however, when the aspect ratio of the DAP elements approaches unity, or when large amounts of longitudinal shear lag are present in the DAP elements. However, the techniques of [7] may be used to capture most shear lag effects.

Because precompression has been shown to be beneficial when it comes to increasing depoling and tensile failure strains, a rough model is needed to estimate the amount of precompression. Too much precompression will either yield the substrate in tension or induce a compressive failure in the piezoceramic. By using the linear coefficient of thermal expansions of the actuator and the substrate, the following relationship may be obtained, assuming no external forces and in-plane precompression strains only:

$$\varepsilon = \frac{2E_a t_a \alpha_a \, \Delta T + E_s t_s \alpha_s \, \Delta T}{2E_a t_a + E_s t_s}. \tag{4}$$

By examining equations (1) and (3), it is clear that externally applied forces and moments may play a significant role increasing or decreasing rotor deflections. One of these moments which directly retards blade pitch motions is the propeller moment. If one considers a typical helicopter rotor blade section at a finite pitch angle, θ, then there exists a couple of chordwise forces which act about the feathering axis to pitch the rotor blade back to zero pitch angle. Considering a rotor blade section with mass density m, rotating at an angular speed Ω, at a finite coning angle β and nondimensional radius x, then the blade pitch angle, θ, may be determined if one considers the blade section inertia about the feathering axis, I_θ, and the effective spring constant about the feathering axis, K_q.

$$\int_0^R [I_\theta \ddot{\theta} - (r\ddot{\beta} - x_I \ddot{\theta}) x_I m + I_\theta \Omega^2 \theta - m\Omega^2 r \beta x_I] \, \mathrm{d}r + K_\theta(\theta - \theta_{con}) = \int_0^R M_a \, \mathrm{d}r. \tag{5}$$

Although this applied moment is detrimental to blade deflections, it is easily countered by the addition of mass

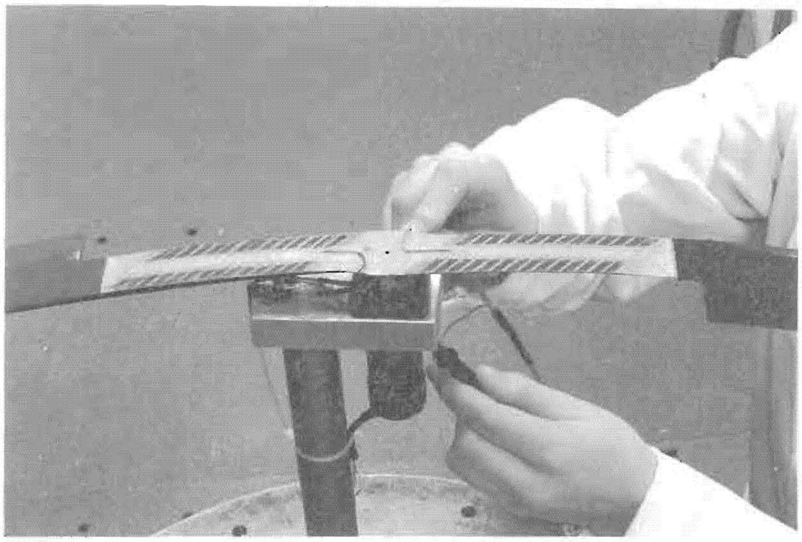

Figure 3. The SSAR during static electrical check.

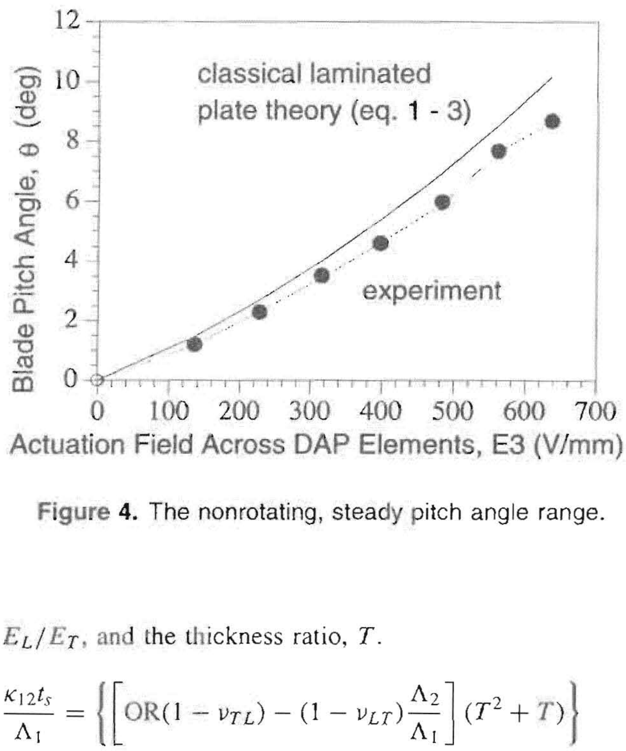

Figure 4. The nonrotating, steady pitch angle range.

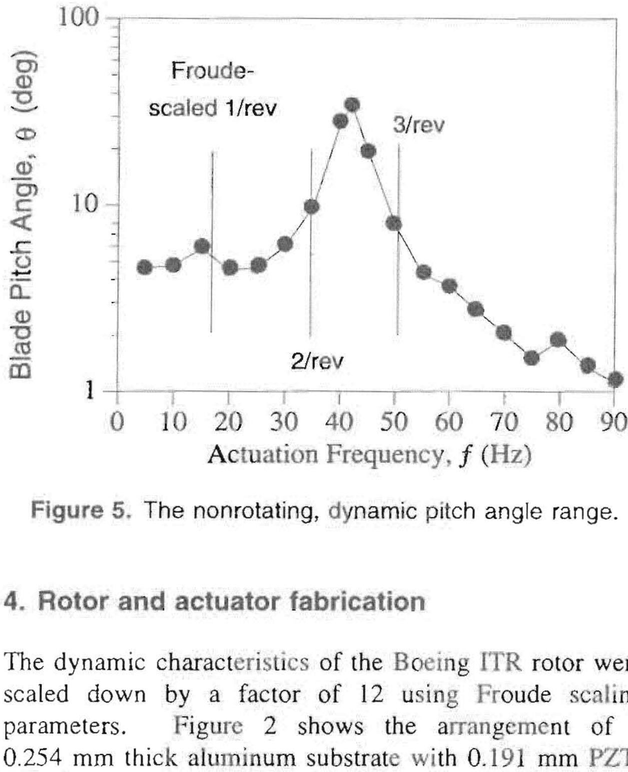

Figure 5. The nonrotating, dynamic pitch angle range.

E_L/E_T, and the thickness ratio, T.

$$\frac{\kappa_{12}t_s}{\Lambda_1} = \left\{\left[\mathrm{OR}(1-\nu_{TL}) - (1-\nu_{LT})\frac{\Lambda_2}{\Lambda_1}\right](T^2+T)\right\}$$
$$\times\left\{\frac{\mathrm{OR}E_sT^3(1-\nu_{LT}\nu_{TL})}{6E_L(1-\nu_s)}\right.$$
$$\left. + (\mathrm{OR}+1-2\,\mathrm{OR}\,\nu_{TL})\left(\frac{T^2}{2}+T+\frac{2}{3}\right)\right\}^{-1}. \quad (8)$$

Clearly, when the orthotropy ratio, OR, and the orthotropic strain ratio, Λ_1/Λ_2, go to unity, or the thickness ratio, T, goes to infinity, the laminate becomes inactive in twist. The first two conditions will occur if conventionally attached piezoelectric (CAP) elements are used. Considering the effective length of the DAP torque plate as L_{eff}, then the steady blade pitch angle follows:

$$\theta = \kappa_{12}L_{eff}. \quad (9)$$

4. Rotor and actuator fabrication

The dynamic characteristics of the Boeing ITR rotor were scaled down by a factor of 12 using Froude scaling parameters. Figure 2 shows the arrangement of a 0.254 mm thick aluminum substrate with 0.191 mm PZT-5H piezoceramic elements bonded on either side. The DAP elements were cut to 0.2 mm tolerances and exhibited an orthotropy ratio in excess of 18 after bonding to the substrate. The elements were fired, poled and mounted in a 177 °C cure using Scotchweld™ adhesive tape. The DAP elements were re-poled after mounting and allowed to age for 1 week.

A 30% attachment area was masked by 25 μm thick Teflon tape placed on the top and bottom of the piezoceramic elements. Brass strips were added to the outer surfaces to act as electrodes. On top of the brass leads, style number 120 fiberglass strips were added to protect the leads from fatigue and mechanical damage as seen in figure 3. Following hub assembly, a pair of 0.25 mm thick graphite–epoxy strips were added below the rotor hub, extending

Alabama EPSCoR Program under contract No NSF-OSR-9550480. The authors would also like to thank Mr Brett Blazer and Mr David Anderson of the Auburn University Materials Engineering Program for helping with the construction of the solid state rotor.

References

[1] Barrett R and Brozoski F 1996 Adaptive flight control surfaces, wings rotors and adaptive aerodynamics *Proc. SPIE Smart Structures and Materials Conf. (San Diego, CA, 1996)* vol 2717, ed I Chopra, pp 178–98

[2] Berry R P 1989 Development and testing of an open-center valve (OCV) pneumatic actuator for the fiber optic guided missile (FOG-M) *US Army Missile Command Technical Report* RD-GC-89-15

[3] Berry R P 1985 Design and development of a closed center valve pneumatic actuator for the fiber optic guided missile (FOG-M) *US Army Missile Command Technical Report* RG-85-1

[4] Barrett R M 1993 Advanced low-cost smart missile fin technology evaluation *Final Report to the USAF Armament Directorate, WL/MNAV, Eglin AFB, FL, by Barrett Aerospace Technologies* F08630-93-C-0039

[5] Barrett R M 1995 Design and manufacturing of adaptive composites for active flight control surfaces *Proc. 2nd Int. Conf. on Composites Engineering (New Orleans, LA, 1995)* ed D Hui (New Orleans, LA: ICCE) pp 53–4

[6] Barrett R, Gross R S and Brozoski F T 1995 Design and testing of subsonic all-moving smart flight control surfaces *Proc. 36th AIAA Structures, Structural Dynamics and Control Conf. (New Orleans, LA, 1995) AIAA Paper* (Washington, DC: AIAA) AIAA-95-1081, pp 2289–96

[7] Barrett R 1992 Active plate and missile wing development using EDAP elements *Smart Mater. Struct.* **1** 214–26

[8] Barrett R 1993 Aeroservoelastic DAP missile fin development *Smart Mater. Struct.* **2** 55–65

[9] Barrett R, Gross R S and Brozoski F 1996 Missile flight control using active flexspar actuators *Smart Mater. Struct.* **5** 121–8

[10] Hanagud S, Roglin R L and NageshBabu G L 1993 Adaptive airfoils for helicopters *Proc. SPIE Smart Structures and Materials Conf. (Albuquerque, NM, 1993)* vol 1917, ed I Chopra, pp 217–24

[11] Barrett R M 1995 Method and apparatus for structural actuation and sensing in a desired direction *US Patent* 5 440 193

[12] Spangler R L and Hall S R 1990 Piezoelectric actuators for helicopter rotor control *31st Structures, Structural Dynamics and Materials Conf. (Long Beach, CA, 1990)* (Washington, DC: AIAA)

[13] Been-Zeev O and Chopra I 1995 Continued development of a helicopter rotor model employing smart trailing-edge flaps for vibration suppression *Proc. SPIE Smart Structures and Materials Conf. (San Diego, CA, 1995)* vol 2443, ed I Chopra, pp 2–19

[14] Giurgiutiu V, Chaudhry Z and Rogers C A 1994 Engineering feasibility of induced-strain actuators for rotor blade active vibration control *Proc. SPIE Smart Structures and Materials Conf. (Orlando, FL, 1994)* vol 2190, ed N Hagood, pp 107–22

[15] Giurgiutiu V, Chaudhry Z and Rogers C A 1994 Active control of helicopter rotor blades with induced strain actuators *35th AIAA/ASME/ASCE/AHS/ASC Structures, Structural Dynamics and Materials Conf. Adaptive Structures Forum (Hilton Head, SC, 1994)* (Washington, DC: AIAA) pp 288–98

[16] Strauß F K and Merkley D J 1995 Design of a smart material actuator for rotor control *Proc. 1995 SPIE Conf. on Smart Structures and Materials (San Diego, CA, 1995)* vol 2443, ed I Chopra, pp 89–104

[17] Crawley E F and De Luis J 1987 Use of piezoelectric actuators as elements of intelligent structures *AIAA J.* **25** 987-97

[18] Crawley E F, Lazarus K B and Warkentin D J 1989 Embedded actuation and processing in intelligent materials *2nd Int. Workshop on Composite Materials and Structures for Rotorcraft (Troy, NY, 1989)*

[19] Crawley E F and Anderson E H 1989 Detailed models of piezoceramic actuation of beams *30th Structures, Structural Dynamics and Materials Conf. (Mobile, AL, 1989)* (Washington, DC: AIAA)

[20] Hagood N W, Kindel R, Ghandi K and Gaudenzi P 1993 Increasing transverse actuation of electroceramics using interdigitated surface electrodes *Proc. SPIE Smart Structures and Materials Conf. (Albuquerque, NM, 1993)* vol 1917, ed N Hagood and G Knowles, pp 341–52

[21] Bent A A, Hagood N W and Rodgers J P 1993 Anisotropic actuation with piezoelectric fiber composites *4th Int. Conf. on Adaptive Structures, (Cologne, 1993)* (Lancaster, PA: Technomics Publishing Co)

[22] Anon. 1990 *Piezo Systems Product Catalog* (Cambridge, MA: Piezo Systems)

[23] Anon. 1991 *A Guide to Modern Piezoelectric Ceramics* (Bedford, OH: Morgan Matroc)

[24] Barrett R 1995 All-moving active aerodynamic surface research *Smart Mater. Struct.* 4 65–74

[25] Jones R M 1975 Micromechanical behavior of a lamina *Mechanics of Composite Materials* (New York: Hemisphere)

[26] Rodgers J P, Bent A A and Hagood N W 1996 Characterization of interdigitated electrode piezoelectric fiber composites under high electrical and mechanical loading *Proc. SPIE Smart Structures and Materials Conf. (San Diego, CA, 1996)* vol 2717, ed I Chopra, pp 642–59

[27] Johnson W 1980 Rotary wing aerodynamics *Helicopter Theory* (Princeton, NJ: Princeton University Press)